

# Developmental and Aging-Related Changes of the Optic Nerve in the Albino Rat: Histological, Histomorphometric and Immunohistochemical Study

Original  
Article

Doaa A. Radwan, Amal K.M El-Kattan, Mona M.M Zoair and Nancy N.A El-Hady Ibrahim

Department of Anatomy and Embryology, Faculty of Medicine, Tanta University, Egypt

## ABSTRACT

**Introduction:** Optic nerves development begins throughout pregnancy and continues after birth. Aging entails gradual degeneration of the structure and the number of the optic nerve axons.

**Aim of the Work:** This research was designed to clarify the prenatal and postnatal development of the optic nerve in the albino rat and the age-related changes in its axons.

**Material and Methods:** Forty-five albino rats were used. The animals were divided into Prenatal group (Group I) and Postnatal group (Group II). In Group I, ten adult males were put with ten females for mating. Pregnant females were sacrificed at different times of gestation and five embryos were extracted for each subgroup; subgroup IA (aged 7 days of gestation), subgroup IB (aged 14 days of gestation) and subgroup IC (aged 21 days of gestation). In Group II, twenty-five albino rats of different ages were divided into five subgroups; Subgroup IIA (aged one month), Subgroup IIB (aged 3 months), Subgroup IIC (aged 9 months), Subgroup IID (aged 18 months) and Subgroup IIE (aged 24 months). The optic nerves of all subgroups were prepared for histological, immunohistochemical examination. Statistical analysis of immune-positive percentage area and the number of optic nerve axons were performed.

**Results:** Optic nerve was first formed in rat embryos aged 21 days of gestation. It's formed of the axons of retinal ganglion cells. Aging causes apparent deterioration of the optic nerve structure with a highly significant increase in CD31 immunopositive cells percentage area. Ultra-structurally, the number of optic nerve axons significantly decreased.

**Conclusion:** This study provides histological description of development of the optic nerve in the albino rat across different prenatal and postnatal ages. The aging is associated with degeneration, neovascularization and reduction of optic nerve axons which could explain why most elderly have vision loss with varying extent.

**Received:** 27 February 2022, **Accepted:** 14 April 2022

**Key Words:** Aging, CD31, development, optic nerve axons, ultrastructure.

**Corresponding Author:** Doaa A. Radwan, MD, Department of Anatomy and Embryology, Faculty of Medicine, Tanta University, Egypt, **Tel.:** +966 533236020, **E-mail:** dr.doaa.radwan@gmail.com

**ISSN:** 1110-0559, Vol. 46, No. 3

## INTRODUCTION

The optic nerve develops from the optic stalk, which connects the brain to the optic cup. It remains empty till the retinal ganglion cells fibers emerge in the 6<sup>th</sup> week of development. The growth of these fibers gradually obliterates the lumen of the optic stalk and turn it into the optic nerve in the 8<sup>th</sup> week of the development. The glial cells around the optic nerve fibers arise from the inner layer of the optic stalk. The optic nerve's axons begin myelination around the 7<sup>th</sup> month, and it is completed later after delivery<sup>[1,2]</sup>.

About 80% of growth of optic nerve occurs after birth with the greatest linear growth within the first 3 years of postnatal life. From 5 to 15 years, it grows at a slower rate and then stops. This growth pattern is most probably related to the rise in skull size around puberty<sup>[3]</sup>. Several signaling molecules have been involved in directing the optic nerve axons to their target brain nuclei. One of them is the chondroitin sulfate proteoglycans gradients (CSPGs)

which direct axonal growth radially toward the optic nerve and so influence optic axonal growth<sup>[4,5]</sup>.

The optic nerve is divided into several parts: intra-ocular, intra-orbital, intra-canalicular, and intra-cranial. The intra-ocular portion is roughly 1mm long and represents the optic nerve head, where the axons of retinal ganglion cells converge, making it light-insensitive and forming the "blind spot"<sup>[6,7]</sup>. The intra-orbital portion is roughly 25 mm long and goes across the orbital cavity. Because the distance between the posterior globe and the optic foramen is just 20 mm, the optic nerve has an S shape within the orbit. The intra-canalicular part leaves the orbit via the optic foramen located within the lesser wing of the sphenoid then goes through the optic canal (approximately 9 mm in length). The intra-cranial part (about 16 mm long) travels through the cerebral cavity before connecting with the contralateral one to create the optic chiasma<sup>[8,9]</sup>.

Petros *et al.* (2008)<sup>[10]</sup> stated that the axons of retinal ganglion cells forming the optic nerve aren't myelinated

in the retina, but they start to get myelin at the level of the lamina cribrosa, a perforated, sieve-like area of the sclera through which optic nerve fibers emerge. The optic nerve is also composed of neuroglial cells such as astrocytes, microglia and oligodendrocytes. Astrocyte columns and vascular connective tissue septa group the axons into bundles. Moreover, each axon bundle is further divided into fascicles by regular inter-fascicular rows of five or more oligodendrocytes<sup>[11,12]</sup>.

The mammalian eye is similar between rats and humans, with gross and histologic differences due to relative sizing. The average adult rat eye is approximately 4 mm while the human eye measures 23.5–25 mm in diameter. As a result of the rat's small eyes, rats have an enormous depth of focus. In humans, the depth of focus of the unaccommodated eye is from 2.3 meters to infinity. In rats, the depth of focus is from 7 centimeters to infinity<sup>[13,14]</sup>.

Bernstein *et al.* (2016)<sup>[3]</sup> reported that understanding the optic nerve growth is an important in assessing disorders that impact visual function in infants. Moreover, Erdinest *et al.*, (2021)<sup>[15]</sup> had explained that aging is a complex biological process that causes a progressive loss of physiological function, such as vision impairment and degradation of retinal cells and optic nerve fibers. Therefore, the present study was designed to clarify the prenatal and postnatal developmental changes in the albino rat optic nerve axons as well as the effect of aging on their structures. It was performed by histological, histomorphometric and immunohistochemical methods.

## MATERIAL AND METHODS

### Animals

In this study, forty male and female albino rats at different ages were collected from the Animal House, Anatomy Department, Faculty of Medicine, Tanta University. They were kept in separate clean and well aired cages, and they were fed the same laboratory food. The use of animals and methods followed the National Institutes of Health's guidelines for caring for and utilizing laboratory animals (NIH Publications No. 8023, revised 1978) to reduce animal distress and in convenient with the strategies of the Ethical Committee of Medical Research, Faculty of Medicine, Tanta University, Egypt (Approval code: 33908). The animals were divided into two groups:

#### Prenatal group (Group I)

In this group, fifteen adult male and female albino rats (5 males and 10 females) were used. Each one male and two female rats were put in a separate cage for mating. Twenty-four hours later, vaginal smear was taken from each female rat to be examined for the presence of copulation plug. Positive smears indicated the beginning of pregnancy (zero day of pregnancy)<sup>[16]</sup>.

The pregnant females were isolated in the following morning and sacrificed at different times of gestation; after 7, 14 and 21 days of gestation. The contents of their uterine

horns were collected and subdivided into three subgroups (5 animals each) IA, IB and IC at the age of 7, 14 and 21 days of gestation, respectively. The embryos and fetuses of the previous subgroups were decapitated and sections of their heads were done and prepared for histological and immunohistochemical staining to clarify the structure of the eye and optic nerve.

#### Postnatal and aging group (Group II)

In this group, twenty-five rats were divided according to their ages into five subgroups (5 rats each): IIA, IIB and IIC (aged 1, 3 and 9 months respectively; postnatal developmental subgroups), IID and IIE (aged 18 and 24 months respectively; aging-related subgroups). The rats of the previous subgroups were sacrificed at the expected age with a suitable dose of ether.

#### Histological examination

The heads of the rat embryos of the prenatal subgroups as well as the eyeballs and the retrobulbar part of optic nerves at the two sides were separated from the postnatal subgroups. Those on the right side, were fixed in 10% buffered formalin for histological and immunohistochemical studies with hematoxylin and eosin as well as CD31 immunohistochemical staining respectively<sup>[17]</sup>. The anterior segment of the left eyeball was removed resulting in release of the major non-retinal components of the eye and the interior of the eye. The neural retina appeared smooth, opaque and continued with the optic nerve. They were fixed in the 2.5% phosphate buffered gluteraldehyde solution for transmission electron microscopic examination<sup>[18]</sup>.

Finally sacrificed rats were safely collected in a special package according to safety and health precaution measures to be incinerated later. Any unexpected risks appeared during the course of research were cleared to participants and the ethical committee on time.

#### Immunohistochemical examination

The CD31 immunohistochemical stain is a superior angiogenesis marker as the immuno-positive cells are visible in the blood vessel walls. It was carried out in the following manner: The entire eyes were preserved in 10% buffered formalin for 24–36 hours before being infiltrated with 30% sucrose. The retina and retrobulbar optic nerve were sectioned into 5-7 m thick pieces. They were kept at room temperature for 15 minutes and processed for antigen retrieval by digestion in 0.05 % trypsin (pH 7.8). Then they were treated with CD31 monoclonal antibodies and CD31 polyclonal antibodies from mice (platelet endothelial cell adhesion molecule, anti-PECAM-1, and dilution 1:100, Cat. No, A1-82378). Then they were washed three times in phosphate buffered solution (PBS), each for five minutes. The slides were stained for 2-5 minutes with DAB peroxidase substrate (3-3' di-aminobenzidine) until the required intensity was achieved<sup>[19,20]</sup>. The slides from different subgroups were observed and photographed with an Olympus BX50 microscope (Olympus Microsystems,

U-ND6-2, Japan) in Anatomy and Embryology Department, faculty of medicine, Tanta University.

### **Morphometric analysis**

Quantitative study including CD31 percentage area as well as counting the optic nerve axons was performed, then, statistical analysis of the collected data was done.

#### **Estimation of the mean area percentage of CD31 positive cells**

Immunohistochemically quantification of CD31 was conducted by using image analysis software (Image J, 1.46a, NIH, USA). Ten non-overlapping randomly selected fields from each slide were measured at a magnification of 400 for quantitative evaluation of mean area percentage of CD31 positive cells [calculated as the area of positive immunohistochemical reaction \*100/total area]<sup>[21]</sup>.

#### **Counting of optic nerve axons**

In each subgroup, ten low-power electron micrographs of the optic nerve at same magnification, were used for the calculation of cross-sectional area. Samples for counting were photographed at regular intervals within each grid square. The nerve sheath and large peripheral blood vessels were not included in the samples. The axons were counted within a frame of fixed size by Image J's Particle Analyzer. Those axons located within the frame were counted. For each subgroup, the total number of axons in each sample was summed<sup>[22]</sup>.

### **Statistical analysis**

The total number of axons within the optic nerve as well as the data of the CD31 percentage area among all subgroups were expressed as the mean  $\pm$  standard deviation (SD). For multiple comparisons, the statistical difference among all subgroups was assessed by one-way analysis of variance (ANOVA) followed by t-Test to compare pairs of groups. The difference was considered significant when probability of differences (*P value*)  $\leq$  0.05, highly significant if *P value* was less than 0.001. If *P value* was more than 0.05, the difference was considered non-significant<sup>[23]</sup>.

## **RESULTS**

### **Light microscopic results**

#### **Hematoxylin & Eosin Stain**

##### **Retina & optic nerve in prenatal group (Group I)**

Sections in the heads of the embryos aged 7 days of gestation (Subgroup IA) revealed the forebrain with no optic cup protrusion indicating no development of the eye at this age (Figure 1; IA). In the fetuses aged 14 days of gestation (Subgroup IB) the definite shape of the albino rat globe was noticed. The retina consisted of outer pigment epithelial layer and inner thick neuroepithelial layer. However, neither ganglion cells nor axons of the optic nerve could be identified at this age as the optic stalk appeared empty of nerve fibers (Figure 1; IB). At the age of 21 days

of gestation (Subgroup IC), The neuroepithelial layer of the retina was differentiated into outer neuroplastic layer, inner neuroplastic layer and ganglion cell layer. The axons of the ganglion cell layer converged towards the center of the retina forming the optic disc exhibiting a depression on its inner surface (the optic cup). These axons left the retina as the optic nerve with delicate branches of hyaloid artery within it (Figure 1; IC).

##### **Optic nerve in postnatal and aging group (Group II)**

###### **• Subgroup IIA (albino rats aged one month)**

Cross sections in the retro-bulbar part of the optic nerve showed that the optic nerve was ensheathed by three meninges including pia, arachnoid and dura maters from inside outwards. The nerve axons were partially packed with ill-defined nerve bundles. The oligodendrocytes appeared as rounded condensed darkly stained nuclei with clear cytoplasm. The astrocytes exhibited vesicular nuclei with pale eosinophilic cytoplasm (Figure 2; IIA: A&B).

###### **• Subgroup IIB (albino rats aged 3 months)**

The optic nerve was ensheathed by the three well-defined meninges. The nerve axons were closely packed with well-defined nerve bundles. Oligodendrocytes appeared as rounded condensed nuclei with clear cytoplasm and astrocytes exhibited elongated darkly stained nuclei with pale eosinophilic cytoplasm (Figure 2; IIB: A&B).

###### **• Subgroup IIC (albino rats aged 9 months)**

Cross sections in the retro-bulbar part of the optic nerve showed well-defined nerve bundles divided by septa. The oligodendrocytes and astrocytes appeared as the previous age group but vacuolation of the nerve axons began to appear (Figure 2; IIC: A&B).

###### **• Subgroup IID (albino rats aged 18 months)**

The nerve bundles were loosely packed and widely separated with ill-defined meningeal coverings. The oligodendrocytes were degenerated with large vacuolated cytoplasm and the astrocytes exhibited pyknotic nuclei. Vacuolation of nerve axons could be seen inside the nerve bundles (Figure 2; IID: A&B).

###### **• Subgroup IIE (albino rats aged 24 months)**

There were scattered vacuoles containing pale eosinophilic fragmented axons and myelin debris. The oligodendrocytes and astrocytes showed shrunken pyknotic nuclei (Figure 2; IIE: A&B).

### **Immunohistochemical CD31 Stain**

#### **Prenatal group (Group I)**

In Subgroup IB (albino rat fetuses aged 14 days of gestation), sections in the eyeball showed blood vessels distributed in the retina and vitreous humor but no optic nerve axons were observed. In subgroup IC (albino rat fetuses aged 21 days of gestation), blood vessels in the optic nerve axons revealed positive brown coloration of their cells (Figure 3; IB& IC).

**Postnatal group (Group II)**

Subgroups IIA, IIB & IIC (albino rats aged 1, 3 & 9 months) exhibited very small brown coloration (CD31 stain) indicating minute blood vessels in the optic nerve axons. Whereas in subgroups IID & IIE (albino rats aged 18 & 24 months), excessive dense positive cytoplasmic staining of CD31 stain appeared in the cells of the blood vessel walls in the optic nerve in subgroup IID (small blood vessels) and in subgroup IIE (Large blood vessels) (Figure 3; IIA, IIB, IIC, IID & IIE).

**Transmission electron microscopic results****Prenatal group (Group I)**

In Subgroup IC (albino rat fetuses aged 21 days of gestation), cross sections in the optic nerve showed loosely packed axons of different shapes and sizes. Most of them were myelinated and others were unmyelinated. The nerve axons consisted of electron lucent axoplasm that contained mitochondria. The astrocytes were found at the periphery with their processes wrapped around the nerve bundles. The Schwann cells wrapped around the nerve axons. Their nuclei revealed condensed chromatin at the nuclear membrane (Figure 4).

**Postnatal and aging group (Group II)****Subgroup IIA (albino rats aged one month)**

All the axons of the optic nerve were myelinated and compact. The astrocytes were found at the periphery with their processes wrapped around the nerve bundles. The myelinated nerve axons were enclosed within the Schwann cells. They contained elongated nucleus that revealed condensed chromatin at the nuclear membrane with prominent nucleolus. The axoplasm was electron lucent and contained numerous mitochondria (Figure 5; IIA).

**Subgroup IIB (albino rats aged 3 months)**

The myelinated nerve axons were surrounded with thick myelin sheath. In addition to presence of astrocytes and Schwann cells, the oligodendrocytes with their elongated heterochromatic nuclei were found between the myelinated nerve axons. Their cytoplasm contained numerous mitochondria (Figure 5; IIB).

**Subgroup IIC (albino rats aged 9 months)**

There were irregular outlines of the myelinated nerve axons. The Schwann cells exhibited shrunken nuclei with vacuolated cytoplasm and degenerated cristae of the mitochondria. The oligodendrocytes contained heterochromatic nuclei and atrophic cytoplasmic organelles. The axoplasm of some myelinated axons possessed swollen mitochondria and others showed vacuolation or focal myelin damage (Figure 5; IIC).

**Subgroup IID (albino rats aged 18 months)**

The myelinated nerve axons of varying sizes were irregular and distorted in shape. They revealed focal disruption, vacuolation or ballooning of myelin sheath

with increased connective tissue between them. Separation of the lamellae of the myelin sheath appeared within some myelinated nerve axons and swollen mitochondria within some unmyelinated axons. Schwann cells exhibited shrunken nuclei and numerous cytoplasmic vacuoles. Astrocytes possessed elongated pyknotic darkly stained nuclei (Figure 6).

**Subgroup IIE (albino rats aged 24 months)**

Myelinated and unmyelinated optic nerve axons appeared with varying sizes and distorted shapes with appearance of blood vessels among them. Schwann cells surrounding the distorted myelinated and unmyelinated nerve axons showed shrunken nuclei and marked vacuolation in the cytoplasm. Marked degenerative changes of the nerve axons were observed. Some myelinated axons exhibited loss of the axoplasm and swollen mitochondria, others showed marked ballooning and separation of the axoplasm from myelin sheath or exhibited complete loss of the myelin sheath on one side and collection of destructed myelin lamellae at the other side (Figure 7).

**Morphometric and statistical results****Statistical analysis of the mean area percentage of CD31 positive cells in different subgroups**

Statistical analysis of the morphometric results showed a highly significant increase ( $P < 0.001$ ) in the area percentage of CD31 positive immunoreaction in subgroup IC as compared with subgroup IB. Meanwhile, subgroup IIA showed a non-significant ( $P > 0.05$ ) difference in immunoreactivity as compared to either the subgroup IIB or IIC. On the other hand, there was a highly significant difference between subgroup IC&IID, IC&IIE, IIA&IID and IIA&IIE. In addition, there was a highly significant ( $P < 0.001$ ) increase in the area percentage of CD31 positive immunoreaction in subgroup IIE as compared with subgroup IID (Table 1, Histogram 1).

**Statistical analysis of the mean number of axons in the optic nerve in different subgroups**

The mean number of optic nerve axons in albino rat fetus at the age of 21 days (subgroup IC) was  $29.3 \pm 10$ . In rats of subgroups IIA and IIB aged 1 month and 3 months, the mean number of optic nerve axons increased to  $31 \pm 14.6$  and  $33 \pm 22.3$  respectively with no significant difference between both or between them and the prenatal subgroup. This increase was significantly decreased again ( $P < 0.001$ ) in the axons of old albino rats of subgroups IIC (aged 9 months), IID (aged 18 months) and IIE (aged 24 months). Their mean axon numbers were  $28.7 \pm 11.3$ ,  $8.8 \pm 3.3$  and  $7 \pm 2.9$  respectively with non-significant difference between IID & IIE. There was a highly significant difference between subgroup IC&IID, IC&IIE, IIA&IID and IIA&IIE. On the other hand, there was a significant difference between other subgroups (Table 2, Histogram 2).

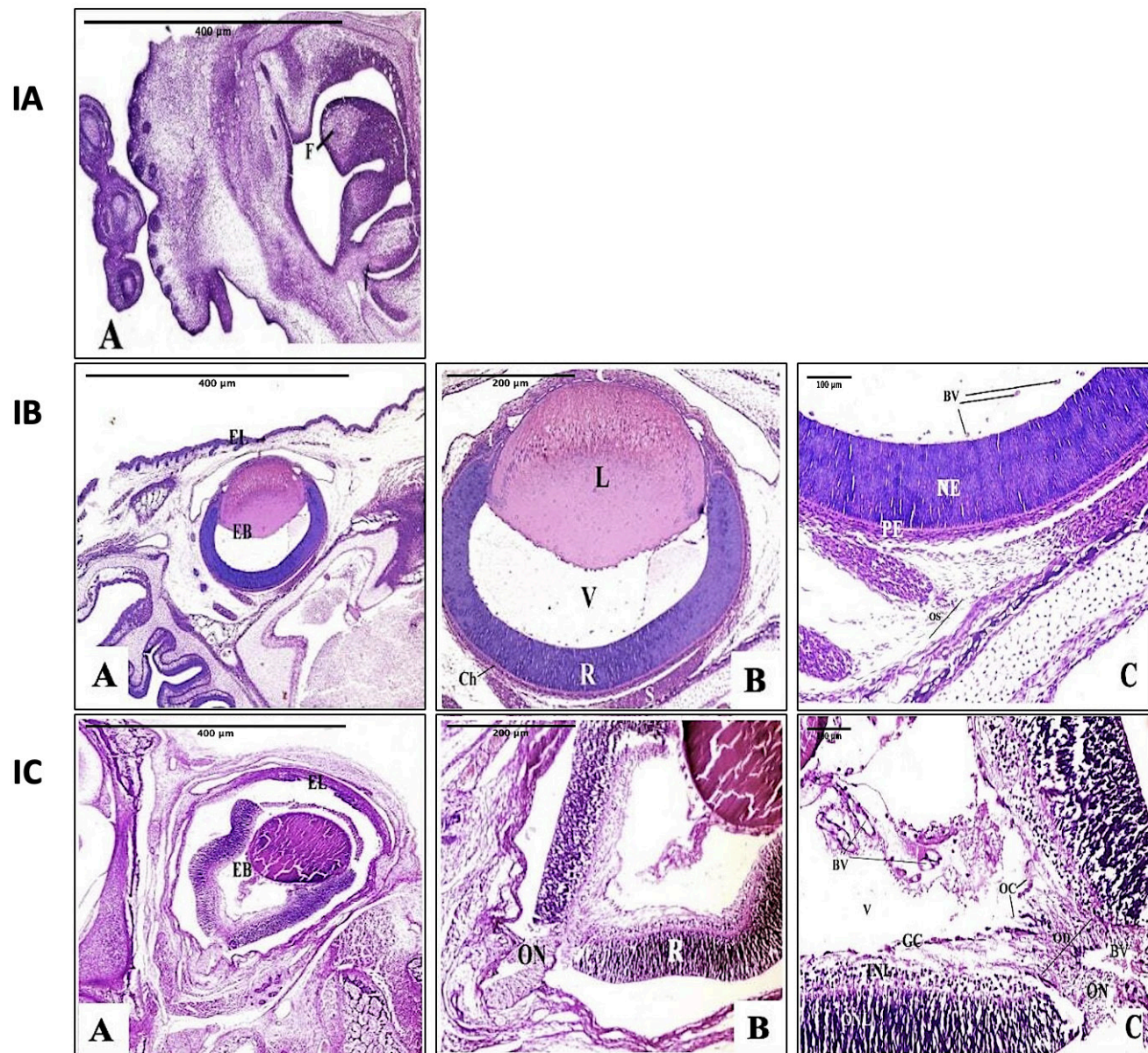


**Fig. 1:** Photomicrographs of sections in the heads of albino rat embryos and fetuses at different ages showing:

- In embryos aged 7 days of gestation (IA), the forebrain (F) appears with no optic cup protrusion indicating no development of the eye at this age.
- In fetuses aged 14 days of gestation (IB) the layers of the eyeball (EB) and the eye lids (EL) are well defined. The outer layer includes the sclera (S) and the cornea (C). The second layer includes the choroid (Ch) and the iris (I). The inner layer represents the retina (R). The vitreous humor (V) can be observed between the lens (L) and the retina. The retina consists of outer pigment epithelial layer (PE) and inner thick neuroepithelial layer (NE). The optic stalk (OS) appears empty of nerve fibers and many vitreous blood vessels (BV) are noticed.
- In fetuses aged 21 days of gestation (IC), the eyelids (EL) and the eyeball (EB) appear with the optic nerve (ON) emerges from the posterior pole of the retina (R). The neuroepithelial layer of the retina is differentiated into outer neuroplastic layer (ONL), inner neuroplastic layer (INL) and ganglion cell layer (GC). The axons of the ganglion cells converge at the posterior pole of the eye forming the optic disc (OD) with a depression on its inner surface forming the optic cup (OC). Delicate blood vessels (BV) are distributed in the vitreous humor (V) and within the optic nerve (ON) (Hx.& E. AX40, BX100 & CX200).

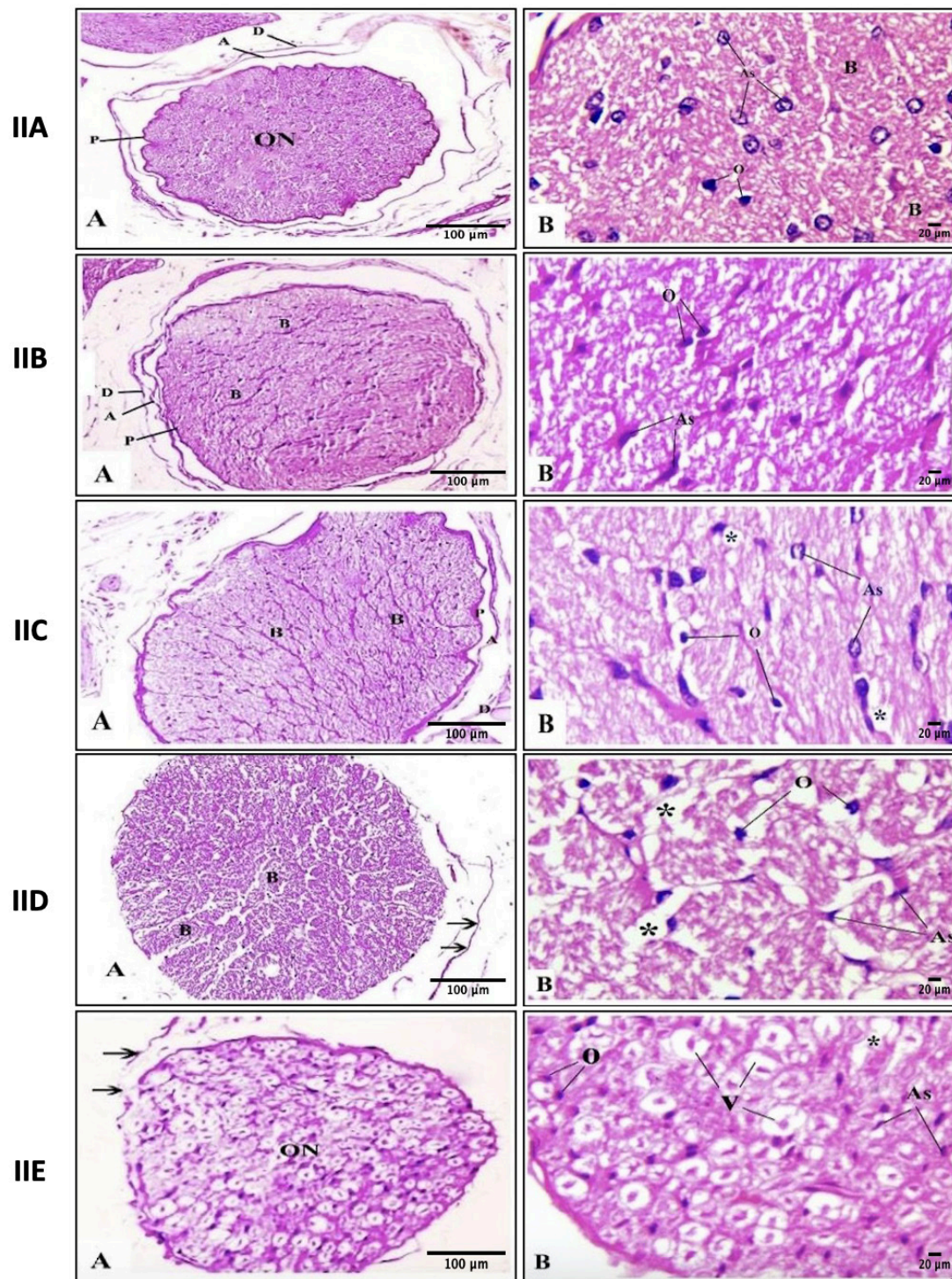


**Fig. 2:** Photomicrographs of cross sections in the retro-bulbar part of the optic nerves of albino rats at different ages showing:

- In the rats aged 1-month (IIA), the optic nerve (ON) is surrounded by three layers; the pia (P), arachnoid (A) and dura (D) maters from inside outwards. Ill-defined bundles (B) of the optic nerve axons are seen. The oligodendrocytes (O) appear as condensed darkly stained nuclei with clear cytoplasm and the astrocytes (As) exhibit pale eosinophilic cytoplasm with vesicular nuclei.
- In the rats aged 3 months (IIB), the three meninges are well-defined. The nerve axons are closely packed with well-defined nerve bundles (B). Higher magnification shows the oligodendrocytes (O) with small rounded condensed nuclei and clear cytoplasm. The astrocytes (As) exhibit elongated darkly stained nuclei with pale eosinophilic cytoplasm.
- In the rats aged 9 months (IIC), well-defined bundles (B) of the nerve fibers can be seen divided by septa. The oligodendrocytes (O) and astrocytes (As) appear normal however vacuolation (\*) of the nerve axons can be noticed.
- In the rats aged 18 months (IID), the meningeal coverings (arrows) are ill defined. Nerve bundles (B) are loosely packed and widely separated. Degenerated oligodendrocytes (O) appear with large vacuolated cytoplasm and astrocytes (As) show pyknotic nuclei with more vacuolations (\*) inside the nerve bundles.
- In the rats aged 24 months (IIE), scattered vacuoles (V) containing pale eosinophilic fragmented axons and myelin debris are noticed. The oligodendrocytes and astrocytes show shrunken pyknotic nuclei (Hx.& E.: AX200 & BX1000).

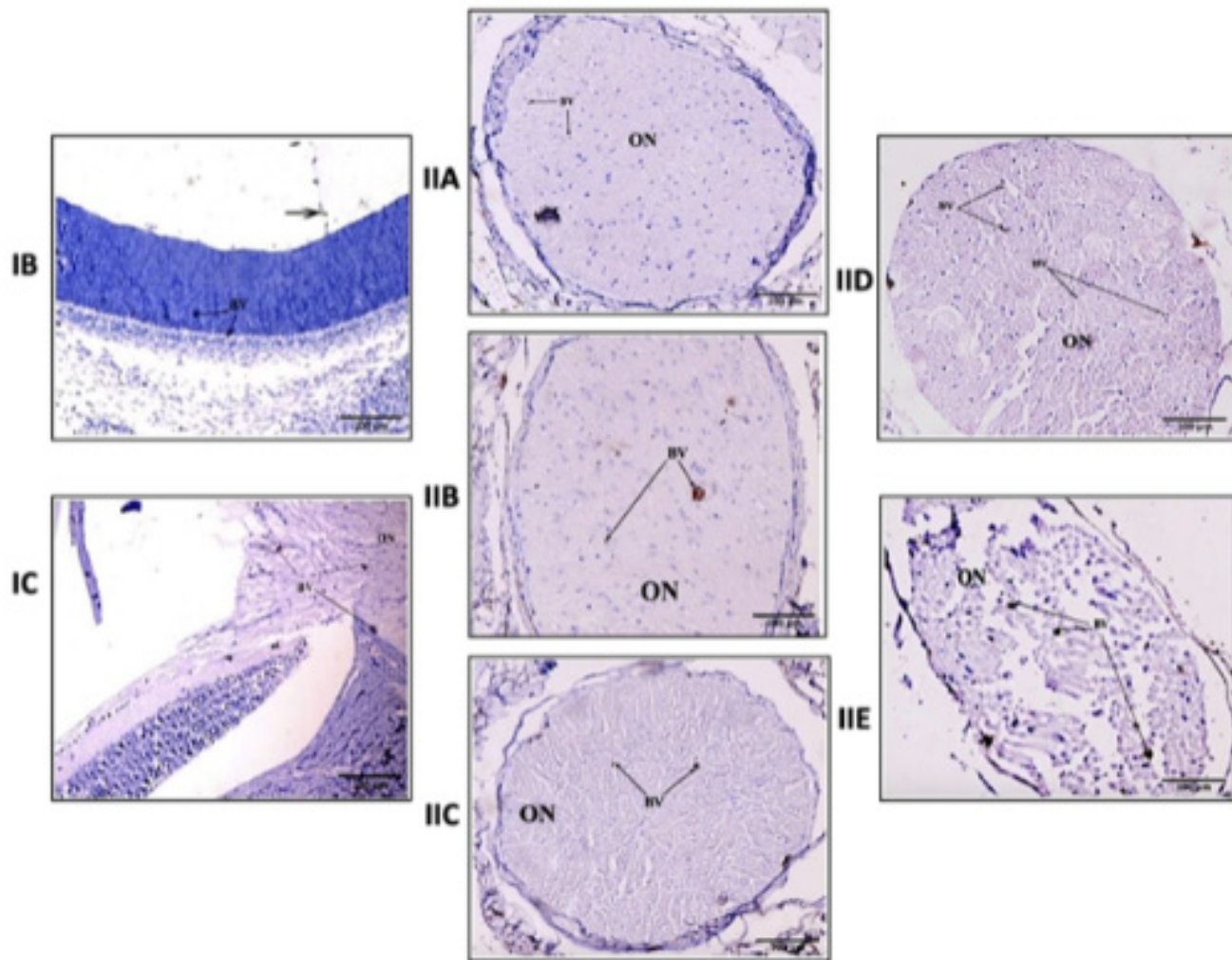


**Fig. 3:** Photomicrographs of cross sections in the eyeball and optic nerve (ON) of albino rats at different ages showing:

- In fetuses aged 14 days of gestation (IB), brown coloration of blood vessels (BV) distributed in the retina and vitreous humor (arrows) but no optic nerve axons are observed.
- In fetuses aged 21 days of gestation (IC), brown coloration is noticed in the cells of blood vessels (BV) in optic nerve axons (ON).
- In the optic nerve sections of 1 (IIA), 3 (IIB) and 9 (IIC) months aged albino rats, very small brown coloration indicating minute blood vessels (BV)
- In the optic nerve sections of 18 (IID) and 24 (IIE) months aged rats, excessive dense positive cytoplasmic staining of CD31 in the cells of the blood vessel walls (BV) appears in the optic nerve in both subgroup IID (small blood vessels) and in subgroup IIE (large blood vessels) (CD31 immunostaining X 200)

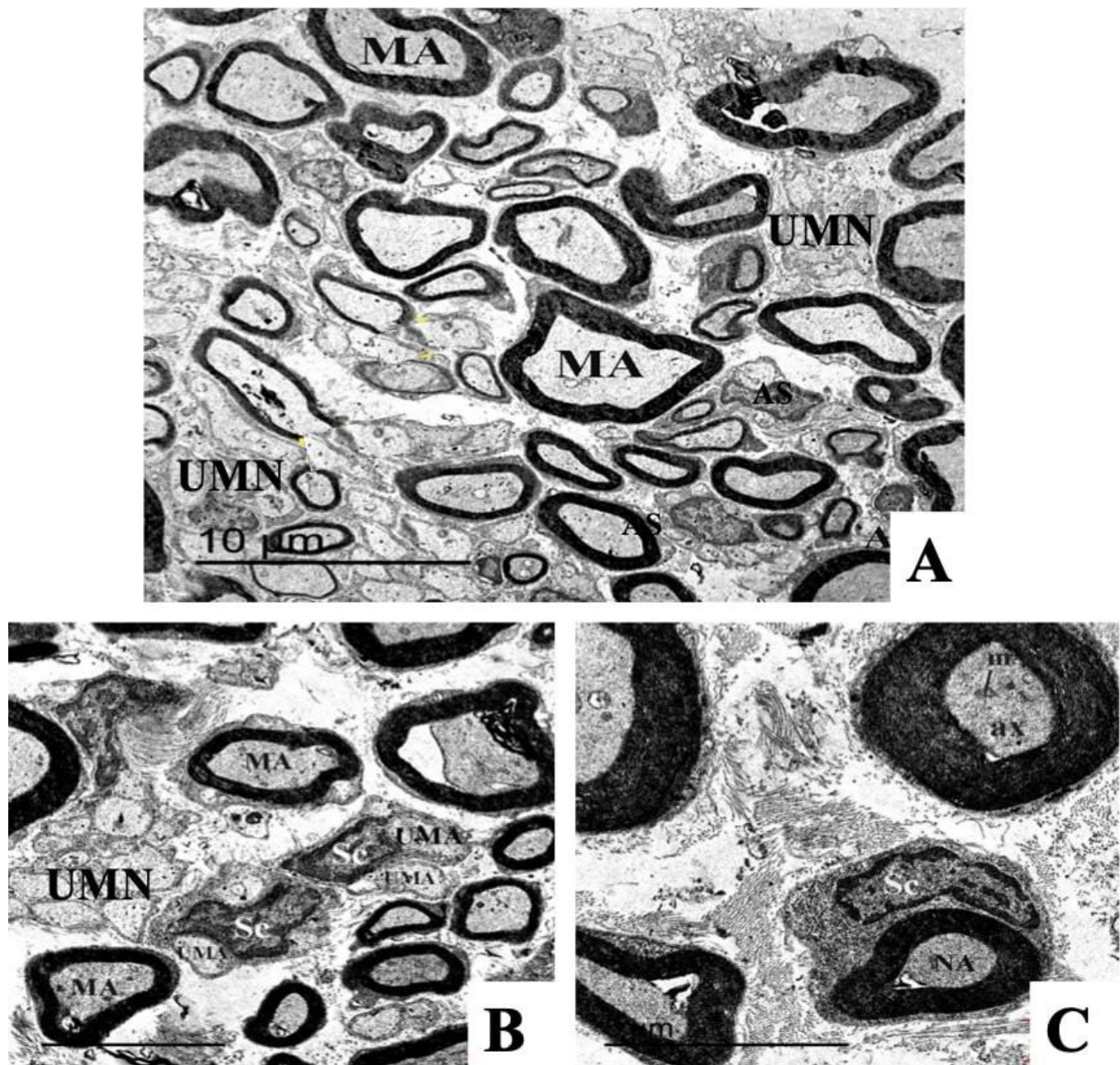


**Fig. 4:** Electron micrographs in optic nerve cross sections of 21 days aged albino rat fetus (Subgroup IC) showing loosely packed axons of different shapes and sizes. Most of them are myelinated (MA) and some are unmyelinated (UMA). The astrocytes (AS) are found at the periphery wrapping around the nerve bundle. The Schwann cell (Sc) wraps around optic nerve axons (NA). Its nucleus reveals condensed chromatin at the nuclear membrane. The nerve axons consist of electron lucent axoplasm (ax) and contain mitochondria (m) (TEM AX 600, B X1200 & CX1500)

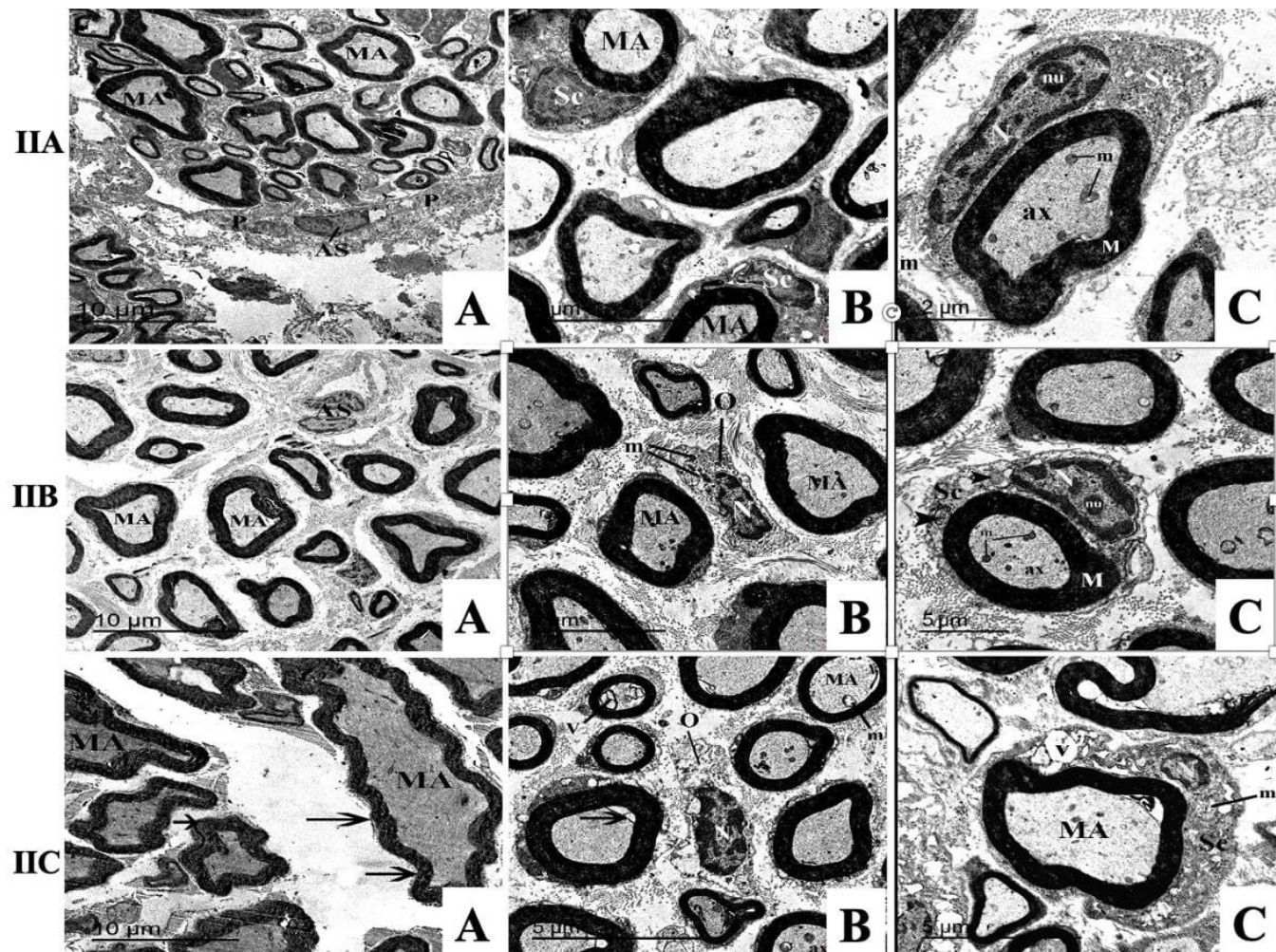


**Fig. 5:** Electron micrographs in optic nerve cross sections of albino rats at different ages showing:

- In rats aged 1 month (IIA), most nerve axons are myelinated (MA) and compact. The astrocytes (AS) are found at the periphery with their processes (P) wrap around the nerve bundle. The myelinated nerve axon (MA) is surrounded with thick myelin sheath (M) and enclosed in Schwann cell (Sc) whose nucleus (N) appears elongated with a prominent nucleolus (nu) and its cytoplasm contains mitochondria (m). The axoplasm (ax) is electron lucent and contains numerous mitochondria (m).
- In rats aged 3 months (IIB), in addition to astrocytes (AS) and Schwann cell (Sc), oligodendrocytes (O) are noticed with their elongated heterochromatic nuclei (N) between the myelinated optic nerve axons (MA). Their cytoplasm contains numerous mitochondria (m).
- In rats aged 9 months (IIC), the myelinated nerve axons (MA) begin to possess irregular outlines (arrows). Oligodendrocytes (O) appear with heterochromatic nuclei (N) and atrophic cytoplasmic organelles. The axoplasm (ax) of some myelinated axons possesses swollen mitochondria (m) and others show vacuolation (V) or focal myelin damage (arrow). Schwann cell (Sc) around the myelinated axons (MA) appears with a shrunken nucleus (N), a vacuolated (V) cytoplasm and degenerated cristae of the mitochondria (m) (TEM AX600, BX1200 & C: IIA, IIC X1500 and IIBX 2500).

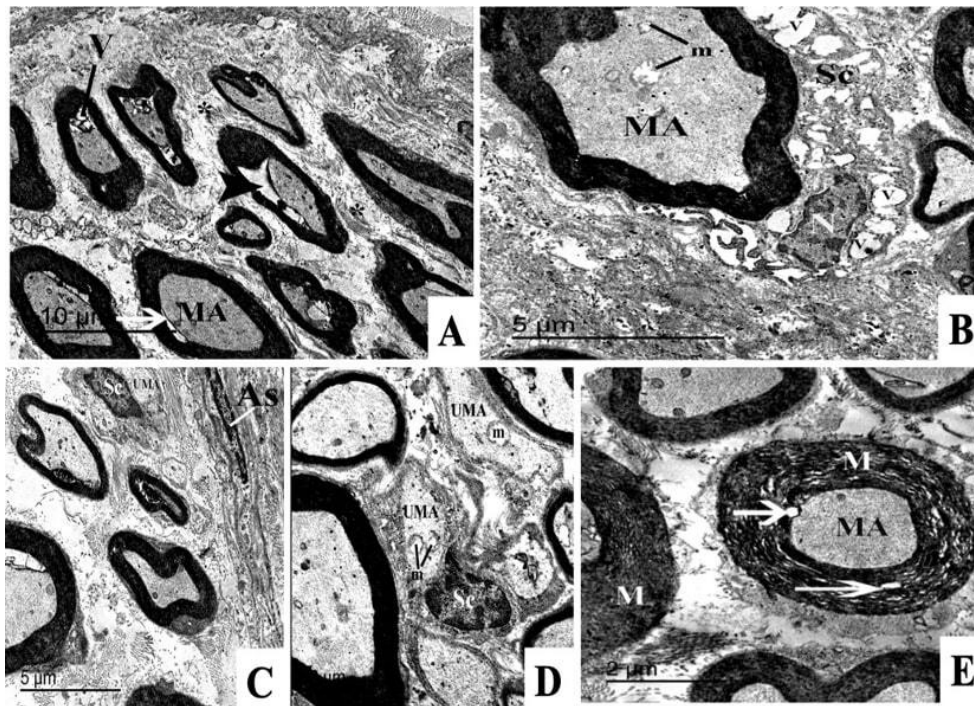


**Fig. 6:** Electron micrographs in optic nerve cross sections of 18 months aged albino rats (IID) showing irregular distorted myelinated nerve axons (MA) of varying sizes with increased connective tissue (\*) between them. They reveal focal disruption (arrow), vacuolation (V) or ballooning (arrowhead) of myelin sheath and destructed cristae of their mitochondria (m). Some myelinated nerve axons (MA) show separation of the lamellae (arrows) of the myelin sheath (M) and some unmyelinated nerve axons (UMA) show swollen mitochondria (m) with destructed cristae. Schwann cells (Sc) surrounding the irregular myelinated nerve axons exhibit shrunken nuclei (N) and numerous cytoplasmic vacuoles (V). An astrocyte (AS) is noticed with elongated pyknotic darkly stained nucleus (TEM AX600, BX1500, CX1200, DX2000 & EX2500).

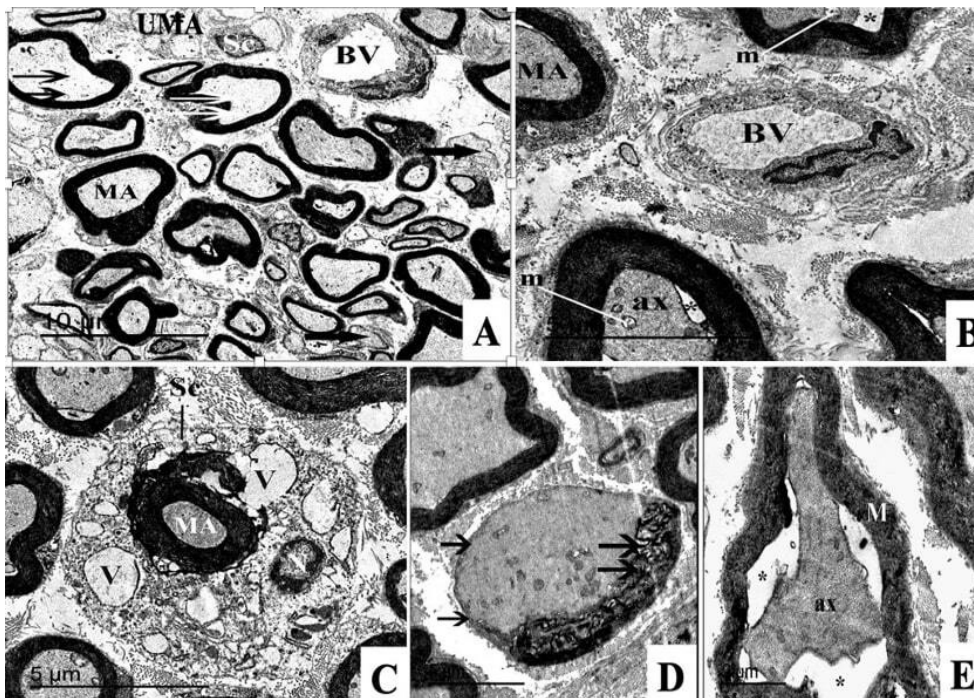


**Fig. 7:** Electron micrographs in an optic nerve cross sections of 24 months aged albino rats (IIE) showing myelinated (MA) and unmyelinated (UMA) axons of varying sizes and distorted shapes. Blood vessels (BV) are detected between the myelinated nerve axons. Some myelinated axons exhibit atrophic Schwann cells (Sc) with shrunken nuclei (N) and marked vacuolation (V) in the cytoplasm. Some of them exhibit complete loss of the myelin sheath on one side (arrows) and collection of destructed myelin lamellae at the other side (double arrows). Others show swollen mitochondria (m) or marked ballooning and separation (\*) of the axoplasm (ax) from myelin sheath (M) (TEM; AX 600, BX 1500, CX 1200, DX 2000 & Ex2500).

**Table 1:** The CD31 positive immunostaining percentage area expression and their statistical comparison in the different subgroups.

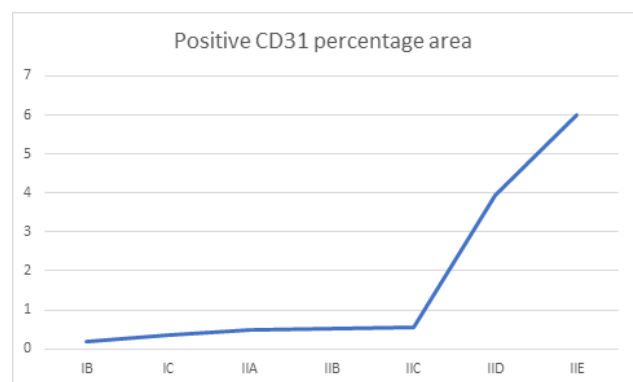
Subgroups	CD31 percentage area		ANOVA							
	Range	Mean ± SD	F	P-value						
IB	0.143 - 0.211	0.179± 0.024	618.9	< 0.001**						
IC	0.245 - 0.422	0.354± 0.057								
IIA	0.402- 0.576	0.505± 0.048								
IIB	0.411- 0.591	0.511± 0.067								
IIC	0.431- 0.599	0.54± 0.061								
IID	3.265 - 4.927	3.95± 0.526								
IIE	5.231 - 7.213	6.012± 0.555								
t-Test										
IB&IC	IB&IIA	IB&IIB	IB&IIC	IB&IID	IB&IIE	IC&IIA	IC&IIB	IC& IIC	IC&IID	IC&IIE
<0.001**	<0.001**	<0.001**	<0.001**	<0.001**	<0.001**	<0.001**	<0.001**	<0.001**	<0.001**	<0.001**
IIA&IIB	IIA&IIC	IIA&IID	IIA&IIE	IIB&IIC	IIB&IID	IIB&IIE	IIC&IID	IIC&IIE	IID&IIE	
0.825	0.176	<0.001**	<0.001**	0.328	<0.001**	<0.001**	<0.001**	<0.001**	<0.001**	

SD=standard deviation, P-value > 0.05 means no significant difference and P-value ≤ 0.001 means highly significant difference (\*\*).

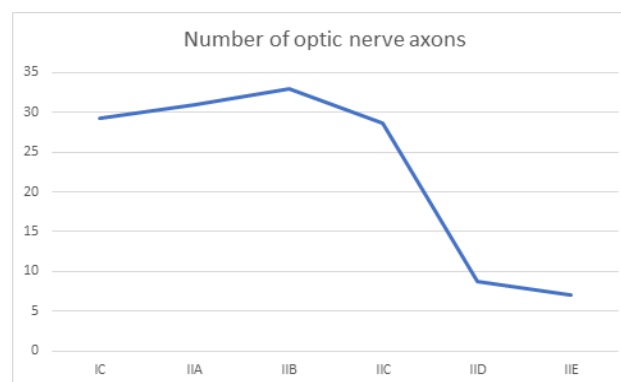
**Table 2:** The mean number of optic nerve axons and their statistical comparison in the different subgroups

Subgroups	Axon numbers		ANOVA				
	Range	Mean ± SD	F	P-value			
IC	15-45	29.3± 10	7.176	< 0.001**			
IIA	10-60	31± 14.6					
IIB	13-85	33± 22.3					
IIC	10-45	28.7± 11.3					
IID	4-15	8.8± 3.3					
IIE	4-12	7± 2.9					
t-Test							
IC&IIA	IC&IIB	IC&IIC	IC&IID	IC&IIE	IIA&IIB	IIA&IIC	IIA&IID
0.4	0.5	0.004*	<0.001**	<0.001**	0.3	0.06*	0.001**
IIA&IIE	IIB&IIC	IIB&IID	IIB&IIE	IIC&IID	IIC&IIE	IID&IIE	
0.001**	0.04*	0.004*	0.003*	0.01*	0.01*	0.1	

SD=standard deviation, P-value > 0.05 means no significant difference, P-value ≤ 0.05 means significant difference (\*) and P-value ≤ 0.001 means highly significant difference (\*\*).



**Histogram 1:** Positive CD31 percentage area in the different subgroups



**Histogram 2:** The number of the axons of the optic nerve in the different subgroups

## DISCUSSION

The vertebrate retina has been widely used as a model for studying the central nervous system's development. Because of its accessibility and relatively simple organization, it may be used to investigate basic functions such cell proliferation, differentiation, and death<sup>[24]</sup>.

Grossniklaus *et al.* (2013)<sup>[25]</sup> reported that the structure of the optic nerve changes with age. These changes included progressive ganglion cell loss; the precursor of optic nerve axons and optic nerve degeneration. Therefore, the current study aimed to clarify the prenatal and postnatal age-related changes in the albino rat optic nerve structure and number of axons.

In this study, albino rats at different ages were used. The ages of the prenatal group were 7, 14 and 21 days of gestation while those of the postnatal and aging groups were 1, 3, 9, 18 and 24 months. These animal ages were chosen based on the equivalence with human<sup>[26,27]</sup>. Roughly, 21 to 30 days old rats would be equivalent to 6 months old child, 2 to 3 months old rats to 14 to 20 years old human, 6 to 9 months old rats to 18 to 30 years old human, 15 to 18 months old rats to 40 years old human and 22 to 24 months old rats to 60 years old human<sup>[28,29]</sup>.

In the present work, embryos at a gestational age of 7 days (subgroup IA) showed no development of the eye. On the other hand, in the fetuses aged 14 days of gestation (subgroup IB) the globe became well defined and their retinae consisted of two layers of cells; outer pigment epithelial layer and inner thick neuroepithelial cell layer. Neither ganglion cells nor axons of the optic nerve could be observed in this age. This result was confirmed by Cruchten *et al.* (2017)<sup>[30]</sup> who mentioned that the bundles of optic nerve axons were observed only in rats at GD14.5 to 15, when the first axons from the ganglion cells appear.

At the age of 21 days of gestation (subgroup IC) of the retina, this work reported that the thick neuroepithelial layer of the retina was differentiated into outer neuroblastic and inner neuroblastic layers with appearance of new layer of ganglion cells. Ilia & Jefferey (1996)<sup>[31]</sup> explained that to be due to melanin or an associated product in the retinal pigment epithelium (RPE) that influences the birth dates of ganglion cells in the retina of the rat. Furthermore, Nguyen-Ba-Charvet & Rebsam (2020)<sup>[32]</sup> explained that different molecular mechanisms, especially the cascade of transcription factors impact the fate of retinal ganglion cells. In subgroup IC, It was also noticed that the axons of ganglion cells emerged on the inner side of the retina then converged towards the center of the retina forming the optic disc and left the retina as the optic nerve. These results coincided with those of Cruchten *et al.* (2017)<sup>[30]</sup> who observed that the nerve fiber layer is formed at GD15 to 16 then continue as the optic nerve.

Ultrastructural examination was done for the optic nerve axons in 21 days aged albino rat fetuses (subgroup IC). They appeared loosely packed with different shapes

and sizes. The majority of them were myelinated, while others were not. These axons were made up of electron-lucent axoplasm with a lot of mitochondria. Schwann cells whose nuclei revealed condensed chromatin at the nuclear membrane were found wrapping around optic nerve axons. Many astrocytes, on the other hand, were located in the periphery, their processes wrapping around each nerve bundle. Burne & Raff (1997)<sup>[33]</sup> suggested that RGC axons induce the astrocyte proliferation. This mitogenic effect of RGCs on optic nerve astrocytes is mediated by neuregulins which may be involved in maturation or survival of astrocytes.

Postnatally, in the present work, the retro-bulbar part of the optic nerves of 1, 3 and 9 months-old albino rats were ensheathed by three meninges; pia, arachnoid and dura maters that became well-defined with the advancement of age. The nerve axons were closely packed with ill-defined nerve bundles in young age and well-defined nerve bundles with increasing age. Ultrastructurally, the nerve axons were enclosed within Schwann cells that contained elongated nuclei with condensed chromatin at the nuclear membrane and prominent nucleoli. The axoplasm contained numerous mitochondria. These findings agree with those observed by Fetouh & Hegazy (2013)<sup>[34]</sup> who assessed the structure of optic nerve in rabbits and found that in young animals, the optic nerve fibres appeared as closely packed myelinated axons of tiny diameters separated by processes of astrocytes while in early adult animals, The optic nerve fibres had the same structure as those of young animals, with the exception that the axons were bigger in diameter. The astrocytes and oligodendrocytes were found with no structural changes in both young and early adult animals.

Vrolyk *et al.* (2017)<sup>[35]</sup> assessed the neonatal and juvenile ocular development in rats and reported that at postnatal day 1 (PND1), the optic nerve was made up of unmyelinated nerve fibers with randomly distributed glial cells including astrocytes and oligodendrocytes. PND10 revealed that mature oligodendrocytes were more abundant and organized in a linear pattern. Axon myelination was completed at PND14.

In the present study, oligodendrocytes were found between the myelinated optic nerve axons only in postnatal groups. They exhibited condensed heterochromatic nuclei and clear cytoplasm containing many mitochondria. The astrocytes were found at the periphery wrapped around the nerve bundles. They revealed vesicular nuclei with pale cytoplasm. These results coincide with that of Zhu *et al.* (2013)<sup>[36]</sup> who reported that the glial tissue between the nerve fibers formed glial septa in the form of trabeculae containing capillaries. Butt *et al.* (2004)<sup>[37]</sup> stated that oligodendrocytes were responsible for production of myelin sheaths that insulate axons while astrocytes modulated the metabolism and potassium homeostasis. Walling & Marit (2016)<sup>[38]</sup> reported that axon myelination begins at PND8 (post-natal day 8) adjacent to the optic disc and the optic chiasma and is completed between PND14 and PND16. They explained that myelination was controlled

by intercellular interactions between neurons and glia cells such as oligodendrocytes and astrocytes.

The effect of oligodendrocytes and myelin on axon maturation in the developing rat was investigated by Colello *et al.* (1994)<sup>[39]</sup>. They prevented oligodendrocyte development by destruction of their precursors by unilateral x-irradiation at birth then they measured the axon diameters in both the normal and the myelin-free optic nerves at different ages. Their results demonstrated that the absence of oligodendrocytes reduce the axon diameter growth however, ganglion cells were of similar size, suggesting that ganglion cell growth occurs in spite of the lack of myelin and axon diameter maturation. Almeida & Lyons (2017)<sup>[40]</sup> also reported that neuronal activity influences oligodendrocytes differentiation from the oligodendrocyte progenitor cells and so promoting myelination of the axons that significantly change axonal conduction properties. Conduction along already-myelinated axons may also be mediated by alterations to the axon itself. They highlighted the observations that neuronal activity can rapidly tune axonal diameter.

Aging changes of the optic nerve of albino rats were observed in the present work at 18 and 24 months of age. These changes were moderate at 18 months (subgroup IID) and became extensive at 24 months (subgroup IIE). These changes involved ill-defined meningeal coverings, loosely packed and widely separated nerve bundles and irregular distorted myelinated nerve axons of varying sizes. Schwann cells exhibited shrunken nuclei with vacuolated cytoplasm and degenerated cristae of the mitochondria. Some unmyelinated axons revealed swollen mitochondria while some myelinated axons exhibited loss of the axoplasm and myelin sheath. Similar findings were noticed in the work of Yassa (2014)<sup>[41]</sup> who studied the histology of optic nerve at different ages of male Sprague–Dawley rats and they concluded that the age-related changes of the optic nerve include increase of the optic nerve sheaths (meningeal membranes), decreased number and size of nerve fibers. Myelin disturbances including widening, whorls, splitting and vacuolations of the myelin lamellae were also observed. Fetouh & Hegazy (2013)<sup>[34]</sup> also assessed the structure of optic nerve in late adult and senile rabbits and found that in late adult animals, the optic nerve fibers were closely packed but some depleted areas could be noticed filled by degenerating axons with electron dense axoplasm. In senile animals, there was extensive degeneration of the nerve axons and their myelin sheath. Many astrocytes had pyknotic nuclei and abundant cytoplasmic filaments. The oligodendrocytes had irregular nucleus and their cytoplasm was filled with vacuoles and inclusion bodies.

In this work, among the aging groups (Subgroups IID & IIE), the oligodendrocytes contained heterochromatic shrunken nuclei and atrophic cytoplasmic organelles and the astrocytes possessed elongated pyknotic darkly stained nuclei. Furthermore, in this work, blood vessels could be seen among the nerve axons in albino rats aged 18 and 24 months. Similar findings were noticed in the work of

Tremblay *et al.* (2012)<sup>[42]</sup> and El-sayyad *et al.* (2014)<sup>[43]</sup> who reported that the oligodendrocytes and astrocytes were abnormally damaged throughout the optic nerve tissues in aging rats. Their main pathological findings of oligodendrocytes and astrocytes were nuclear pyknosis. Also, they detected widespread network of capillaries throughout the optic nerve in old age.

The immunohistochemical stain, CD31 is an excellent marker of vascular endothelial cells<sup>[48]</sup>. It is used in the present study and revealed that at the age of 14 days of gestation (subgroup IB), small blood vessels were distributed in the retina but no vessels were noticed among the optic nerve axons. Whereas, at the age of 21 days of gestation (subgroup IC), optic nerve axons were noticed with appearance of brown colouration distributed in the places of the blood vessels. These results agree with those of Hasegawa *et al.* (2008)<sup>[44]</sup> who reported that the initial retinal vasculature develops by vasculogenesis, differentiation and organization of angioblasts with expression of CD39, VEGF, CD34 and CD31.

Postnatally, in subgroups IIA, IIB and IIC, CD31-stained cross sections in the retrobulber part of the optic nerve of one, three and 9 months-aged albino rats respectively showed negative reaction to the stain. On the other hand, dense positive cytoplasmic staining of CD31 was noticed in the region of the blood vessels in optic nerve of subgroup II D (rats aged 18 months) and II E (rats aged 24 months). These results were in agreement with the results of El-sayyad *et al.* (2014)<sup>[43]</sup> and Liu *et al.* (2011)<sup>[45]</sup> who observed neovascularization during old age and increased positive immunostaining of CD31 which reflected micro-vessel density.

In this study, quantitative measurements of the optic nerve axons revealed an increase in their mean number in subgroup IIA (rats aged one month) and IIB (rats aged 3 months) compared to subgroup IC (fetuses aged 21 days of gestation). The increase in the mean number of optic nerve axons was significantly decreased again ( $P < 0.001$ ) in the axons of old albino rats of subgroups IIC (rats aged 9 months), IID (rats aged 18 months) and IIE (rats aged 24 months). Calkins (2013)<sup>[46]</sup> explained the loss of optic nerve axons to be due to retinal ganglion cells (RGCs) degeneration. However, Yassa, (2014)<sup>[41]</sup> reported age-related ganglion cells degeneration but with no loss of the optic nerve axons. On the other hand, Feng *et al.* (2007)<sup>[47]</sup> previously emphasized that the RGC population is not changed with age in rodents or other species.

Furthermore, the percentage area of CD31 immunopositive cells increased among the prenatal groups IB and IC then became within the same range among the adult groups IIA, IIB and IIC then showed highly significant increase in the aging groups IID & IIE indicating neovascularization. These results agree with those of Bolinteanu *et al.* (2006)<sup>[48]</sup> who assessed the possible age-induced alterations in the microcirculation of the optic nerve in rats grouped by age and concluded that there is increase of vascular

parameters of the optic nerve from birth to adulthood. Liu *et al.* (2011)<sup>[45]</sup> explained this neovascularization that the number of EPCs (Endothelial progenitor cells) in the blood increases significantly after optic nerve injury, and the cells can arrive the injured area to repair injured tissue and enhance angiogenesis.

## CONCLUSION

Finally, it could be concluded that the optic nerve axons begin to develop at 14 days of gestation and continue postnatally. Glial cells including astrocytes and oligodendrocytes become more apparent postnatally in the adult groups aged 1, 3 and 9 months. Aging changes of the optic nerve of albino rats were observed at 18 and 24 months of age. These changes involved ill-defined meningeal coverings, loosely packed with widely separated nerve bundles and irregular distorted myelinated nerve axons of varying sizes. Moreover, neovascularization was also clearly apparent.

## CONFLICT OF INTERESTS

There are no conflicts of interest.

## REFERENCES

- Schoenwolf C, Bleyl B, Brauer R and Francis-west H: "Eye" In: Larsen's human embryology. 5th Edition, Chapter 19. Philadelphia. Elsevier. 2015; pp: 500-507.
- Cruchten SV, Vrolyk V, Lepage MFP, Baudon M, Voute H, Schoofs S, Haruna J, Benoit-Biancamano MO, Ruot B and Allegaert K: Pre- and Postnatal Development of the Eye: A Species Comparison. Birth Defects Research, 2017; 109(19): 1540-1567.
- Bernstein SL, Meister M, Zhuo J and Gullapalli RP: Postnatal growth of the human optic nerve. Eye (Lond). 2016; 30(10):1378-1380.
- Atkinson-Leadbeater K, Bertolesi GE, Hehr CL, Webber CA, Cechmanek PB and McFarlane S: Dynamic expression of axon guidance cues required for optic tract development is controlled by fibroblast growth factor signaling. J. Neurosci. 2010;(30):685-693.
- Samuel A, Rubinstein AM, Azar TT, Livne ZB, Kim SH and Inball A: Six3 regulates optic nerve development via multiple mechanisms. BMCID Scientific report. 2016; 6: 20267.
- Cui, M.S.; Naftel, P.; Lynch, C.; Yang, G.; Daley, P.; Haines, E. and Fratkin, D: Atlas of Histology with Functional and Clinical Correlations. "Eye" 1st Edition, Philadelphia. 2011; pp: 223-232.
- Michelessi M, Lucenteforte E, Oddone F, Brazzelli M, Parravano M, Franchi S, Ng SM and Virgili G: "Optic nerve head and fibre layer imaging for diagnosing glaucoma". Cochrane Database Syst. Rev. 2015; 11: 145-167.
- Sadun AA: Anatomy and physiology. In: Yanoff M, Duker JS (eds) Ophthalmology, 2<sup>nd</sup> Ed. St Louis, Mosby. 2004; pp: 945-950.
- Gala F: Magnetic resonance imaging of optic nerve. Indian J Radiol Imaging. 2015; 25(4): 421-438.
- Petros TJ, Rebsam A and Mason CA: Retinal axon growth at the optic chiasma: to cross or not to cross. Annu Rev Neurosci. 2008; 31: 295-315.
- Berry M, Butt AM, Wilkin G and Perry VH: Structure and function of glia. In: Graham DI, Lantos L (eds) Greenfield's neuropathology, 7th Edition. Edward Arnold: Sevenoaks, Kent. 2002; pp: 75-122.
- Standring S: "Special senses" In: Gray's anatomy: The anatomical basis of clinical practice, 41st Edition. Philadelphia. Elsevier. 2015; pp: 624-709.
- Green DG, Powers MK and Banks MS: Depth of focus, eye size and visual acuity. Vision Res. 1980; 20: 827-835.
- Chen C, Zhao Y and Zhang H: Comparative Anatomy of the Trabecular Meshwork, the Optic Nerve Head and the Inner Retina in Rodent and Primate Models Used for Glaucoma Research. Curr. Eye Res. 2016; 33: 1-12.
- Erdinest N, London N, Lavy I, Morad Y and Levinger N: Vision through Healthy Aging Eyes. Vision. 2021; 5: 46.
- Ochiogu IS, Uchendu CN, and Ihedioha JI: A New and Simple Method of Confirmatory Detection of Mating in Albino Rats (*Rattus norvegicus*). Animal Research International. 2006; 3(3): 527-530.
- Suvarna SK, Layton C and Bancroft JD: Bancroft's Theory and Practice of Histological techniques. 8<sup>th</sup> edition. Elsevier. 2019; pp: 40-138.
- Claybon A and Bishop AJR: Dissection of a Mouse Eye for a Whole Mount of the Retinal Pigment Epithelium. J. Vis. Exp. 2011; 48: 2563-2567.
- Ramos-Vara JA and Miller MA: When tissue antigens and antibodies *get along*: revisiting the technical aspects of immunohistochemistry—the red, brown, and blue technique. Veterinary Pathology. 2014; 51(1): 42-87.
- Menon P and Fisher EA: Immunostaining of macrophages, endothelial cells and smooth muscle cells in the atherosclerotic mouse aorta. Methods Mol. Biol. 2015; 1339: 131-148.
- Wang D, Stockard CR, Harkins L, Lott P, Salih C, Yuan K, Buchsbaum D, Hashim A, Zayzafoon M, Hardy R, Hameed O, Grizzle W and Siegal GP: Immunohistochemistry in the evaluation of neovascularization in tumor xenografts. Biotech Histochem. 2008; 83(3-4): 179-189.
- Reynaud J, Cull G, Wang L, Fortune B, Gardiner S, Burgoyne CF and Cioffi GA: Automated Quantification of Optic Nerve Axons in Primate Glaucomatous and Normal Eyes—Method and Comparison to Semi-Automated Manual Quantification. Invest. Ophthalmol. Vis. Sci. 2012; 53(6): 2951-2959.

23. Dawson-Saunders B and Trapp R: Basic and clinical biostatistics (Lang Medical Book). 3rd edition. New York, USA: Mc Grow Hill Medical Publishing Division. 2001; pp: 161-218.
24. Carmona FD, Glosmann M, Ou J, Jimenez R and Collinson JM: Retinal development and function in a blind mole. *Proc. R. Soc. B.* 2010; 277: 1513-1522.
25. Grossniklaus HE, Nickerson JM, Edelhauser HF, Bergman LAMK and Berglin L: Anatomic Alterations in Aging and Age-Related Diseases of the Eye. *Invest Ophthalmol Vis Sci.* 2013; 54: 23-27.
26. Quinn R: Comparing rat's to human's age: how old is my rat in people years. *Nutrition.* 2005; 21: 775-777.
27. Sengupta P: The laboratory rat: relating its age with Human's. *Int. J. Prev. Med.* 2013; 4: 624-630.
28. Prokai L, Prokai-Tatrai K, Perjesi P, Zharikova AD, Perez EJ, Liu R and Simpkins JW: Quinol-based cyclic antioxidant mechanism in estrogen neuroprotection. *Proc. Natl. Acad. Sci. U. S. A.* 2003; 100: 11741-11746.
29. Zhang QG, Raz L, Wang R, Han D, De-Sevilla L, Yang F, Vadlamudi RK and Brann DW: Estrogen attenuates ischemic oxidative damage via an estrogen receptor alpha-mediated inhibition of NADPH oxidase activation. *J. Neurosci.* 2009; 29: 13823-13836.
30. Cruchten SV, Vrolyk V, Lepage MFP, Baudon M, Voute H, Schoofs S, Haruna J, Benoit-Biancamano MO, Ruot B and Allegaert K: Pre- and Postnatal Development of the Eye: A Species Comparison. *Birth defects research.* 2017; 109:1540-1567.
31. Ilija M and Jeffery G: Delayed neurogenesis in the albino retina: evidence of a role for melanin in regulating the pace of cell generation. *Brain Res Dev Brain Res.* 1996; 95(2):176-83.
32. Nguyen-Ba-Charvet KT and Rebsam A: Neurogenesis and specification of retinal ganglion cells. *International journal of molecular sciences.* 2020; 21(2): 451.
33. Burne JF and Raff MC: Retinal Ganglion Cell Axons Drive the Proliferation of Astrocytes in the Developing Rodent Optic Nerve. *Neuron.* 1997; 18: 223-230.
34. Fetouh F and Hegazy AA: Age-Related Changes in Rabbit Optic Nerve: A Morphological Study. *Journal of American Science.* 2013; 9(10):68-77.
35. Vrolyk V, Haruna J and Benoit-Biancamano MO: Neonatal and Juvenile Ocular Development in Sprague-Dawley Rats: A Histomorphological and Immunohistochemical Study. *Veterinary Pathology.* 2017; 55(2) 310-330.
36. Zhu Y, Li LKH, Zhao ATX, Hu PJX, Huang BYH, Qiang YJB and Peng QMX: Necl-4/SynCAM-4 is expressed in myelinating oligodendrocytes but not required for axonal myelination. *PLoS One.* 2013; 8(5): 1110-1123.
37. Butt AM, Pugh M, Hubbard P and James G: Functions of optic nerve glia: axoglial signaling in physiology and pathology. *Eye.* 2004; 18:1110-1121.
38. Walling BE and Marit GB: The eye and Haderian Gland. In: Picut AP, Picut CA, editors. *Atlas of histology of the juvenile rat.* Amsterdam: Elsevier. 2016; pp: 373-394.
39. Colello RJ, Pott U and Schwab ME: The role of oligodendrocytes and myelin on axon maturation in the developing rat retinofugal pathway. *J Neurosci.* 1994; 14(5 Pt 1): 2594-605.
40. Almeida RG and Lyons DA: On Myelinated Axon Plasticity and Neuronal Circuit Formation and Function. *J. Neurosci.* 2017; 37(42):10023-10034.
41. Yassa HD: Age-related changes in the optic nerve of Sprague-Dawley rats: an ultrastructural and immunohistochemical study. *Acta. Histochem.* 2014; 116: 1085-1095.
42. Tremblay ME, Zettel ML, ISON JR, Allen PD and Majewska AK: Effects of Aging and Sensory Loss on Glial Cells in Mouse Visual and Auditory Cortices. *Glia.* 2012; 60(4): 541-558.
43. El-Sayyad HI, Khalifa SA, El-Sayyad FI, AL-Gebaly AS, El-Mansy AA and Mohammed EAM: Aging-related changes of optic nerve of Wistar albino rats. *American AGE Association* 2014; (36): 519-532.
44. Hasegawa TD, McLeod S, Prow T, Merges C, Grebe R and Lutty GA: Vascular Precursors in Developing Human Retina. *Invest Ophthalmol Vis Sci.* 2008; 49(5): 2178-2192.
45. Liu YM, Hu YB, He TG and Yan H: Role of endothelial progenitor cells in optic nerve injury of rats. *Zhonghua Yan Ke. Za. Zhi.* 2011; 47(12):1089-1095.
46. Calkins DJ: Age-related changes in the visual pathways: blame it on the axon. *Invest Ophthalmol Vis Sci.* 2013; (54): 37-41.
47. Feng L, Sun Z, Han H, Zhou Y and Zhang M: No age-related cell loss in three retinal nuclear layers of the Long-Evans rat. *Vis. Neurosci.* 2007; (24): 799-803.
48. Bolintineanu S, Bolintineanu C, Moțoc A and Vaida M: Neovascularization in rat optic nerve. *Oftalmologia.* 2006; 50(4): 95-101.

## المخلص العربي

## التغيرات النموية والمتعلقة بالشيخوخة في العصب البصري في الفأر الأبيض: دراسة نسيجية وقياسية نسيجية ومناعية

دعاء أحمد رضوان، أمال خليل القطان، مني محمد زعير، ناسي ناجي عبد الهادي

قسم التشرييح وعلم الأجنة كلية الطب جامعة طنطا

**المقدمة:** يبدأ نمو الأعصاب البصرية طوال فترة الحمل ويستمر بعد الولادة. واثناء الشيخوخة يحدث انحطاط تدريجي في تركيب وعدد محاور العصب البصري.

**الهدف من البحث:** تم تصميم هذا البحث لتوضيح التطور قبل الولادة وبعد الولادة للعصب البصري في الجرذ الأبيض والتغيرات المرتبطة بالعمر في محاوره.

**المواد والطرق:** تم استخدام خمسة وأربعين جرذاً من الجرذان البيضاء. تم تقسيم الحيوانات إلى مجموعة ما قبل الولادة (المجموعة الأولى) ومجموعة ما بعد الولادة (المجموعة الثانية).

في المجموعة الأولى، تم وضع عشرة ذكور مع عشر إناث للتزاوج. تم ذبح النساء الحوامل في أوقات مختلفة من الحمل وتم استخراج خمسة أجنة لكل مجموعة فرعية؛ المجموعة الفرعية ١ - أ (عمر ٧ أيام من الحمل)، المجموعة الفرعية ١ - ب (عمر ١٤ يوماً من الحمل) والمجموعة الفرعية ١ - ج (عمر ٢١ يوماً من الحمل).

في المجموعة الثانية، تم تقسيم خمسة وعشرين جرذاً أبيض من مختلف الأعمار إلى خمس مجموعات فرعية. المجموعة الفرعية ٢ - أ (بعمر شهر واحد)، المجموعة الفرعية ٢ - ب (بعمر ٣ أشهر)، المجموعة الفرعية ٢ - ج (بعمر ٩ أشهر)، المجموعة الفرعية ٢ - د (بعمر ١٨ شهراً) والمجموعة الفرعية ٢ - هـ (بعمر ٢٤ شهراً). تم تحضير الأعصاب البصرية من جميع المجموعات الفرعية للفحص النسيجي والكيميائي المناعي. تم إجراء التحليل الإحصائي للنسبة المئوية الإيجابية لصبغة السي دي ٣١ المناعية وعدد محاور العصب البصري.

**النتائج:** تم تكوين العصب البصري لأول مرة في أجنة الفئران التي تبلغ من العمر ٢١ يوماً من الحمل. وقد وجد إنها تتكون من محاور عصبية لخلايا العقدة الشبكية. الشيخوخة تسبب تدهور واضح في بنية العصب البصري مع زيادة النسبة المئوية للخلايا الإيجابية للصبغة المناعية سي دي ٣١. أما من الناحية الهيكلية، فقد لوحظ انخفاض عدد محاور العصب البصري بشكل كبير.

**الاستنتاج:** تقدم هذه الدراسة وصفاً نسيجياً لتطور العصب البصري في الجرذ الأبيض عبر مختلف الأعمار قبل الولادة وبعدها. الشيخوخة مرتبطة بالتناقص في تركيب العصب البصري وتكوين الأوعية الدموية الجديدة.